

2D Direct Numerical Simulation of Intermediate Species Diffusion in Low Temperature Oxidation Process

Atsushi Teraji¹, Takahiro Morikawa², Takashi Ishihara², Yukio Kaneda²

¹Nissan Motor Co., Ltd., Kanagawa, Japan

²Nagoya University, Aichi, Japan

1 Introduction

There are strong demands today for further improvement of the efficiency of internal combustion engines amid growing concerns about the environments. In this regards, homogeneous charged compression ignition (HCCI) engine of which combustion occurs under lean condition is hoped for high efficiency and low emissions. The compression ignition is the complex phenomena including many factors such as chemical reaction, thermal diffusion and fluid mechanics. The controls of the start and combustion speed are key factors for HCCI engine. To make these factors clear, numerical analysis is studied. One is to build chemical kinetic mechanism for understanding essential reaction path and important species in the reaction process. Another is computational fluid dynamics (CFD) to reveal physical factors. The purpose of this article is to understand the diffusion of intermediate species having different diffusion coefficients. It is known that the ignition is affected by a small amount of OH radical which has larger diffusion coefficient than other heavy species. In this study, 2D DNS was carried out to investigate the influence of the intermediate specie diffusion on the ignition delay time and the chemical reaction process. As for reaction mechanism applied for 2D DNS, simplified mechanism was used for the analysis focusing on the high and low diffusion coefficient.

2 Numerical Calculation Method

A compressive Navier-Stokes equation was used as a basic equation. Temporal integration was performed with the fourth-order Runge-Kutta method. The spatial discretization was done by using a eighth-order central difference scheme [2], and the transfer functions of the eighth-order low-pass spatial filter [3] was applied to remove high wavenumber content. The enthalpy h_m , the specific heat c_p and the entropy s_m of each chemical species were derived from chemkin thermodynamic database, and Lewis number Le_m of each species and the binary diffusion coefficient between any two species were derived by the viscosity of the individual species estimated by Chapman-Enskog theory [4]. The Tsushima mechanism [1] which contains 38 reactions and 33 chemical species was used for n-heptane in this study. This mechanism is able to represent the ignition delay with high accuracy and low cost.

All simulations were conducted with two dimensional 4.0×4.0 mm square and 512×512 uniformly distributed rectangular grid. The periodic boundary conditions were assumed in all spatial directions. The

Table 1: Initial turbulence condition

Re_l	u'_{rms}	l	$L_x \times L_y$	$N_x \times N_y$
128.4	8.5 [m/s]	1.0 [mm]	4.0 × 4.0 [mm]	512 × 512

Table 2: Initial condition

ϕ	Pressure	T_{ave}	T'	T_{rms}	Integral scale
0.5	4.0 [MPa]	780 [K]	15 [K]	5.4 [K]	1.0 [mm]

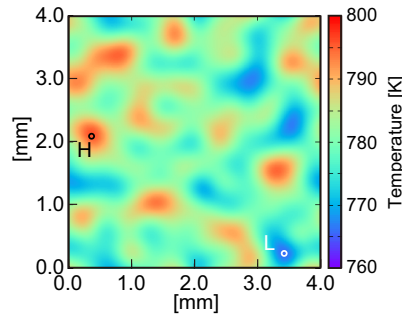


Figure 1: Initial temperature distribution for 2D direct numerical simulation

integral scale of 1.0 mm and an incompressible random flow field with a rms fluctuation velocity u'_{rms} of 8.5 m/s were given for initial turbulence condition as shown in Table 1. As for the initial condition of temperature and pressure, analysis results of temperature measurement and large eddy simulation (LES) by Bai et al. [5, 6] were referred as shown in Table 2. The initial temperature distribution is shown in Fig. 1.

3 Analysis of ignition delay time

First of all, the influence of temperature distribution and turbulence on the temperature history was investigated along with a comparison of temperature history between 0D and 2D calculation results. The temperature histories at the high temperature point H and the low temperature point L in Fig. 1 were investigated respectively. The each temperature histories are shown in Fig. 2 with 0D calculation results. The initial temperature of high and low temperature points were respectively given 795 K and 765 K then. Here, the points of high and low temperature were not fixed under turbulence condition. The maximum and minimum temperature points were plotted after a confirmation of non-fragment lines

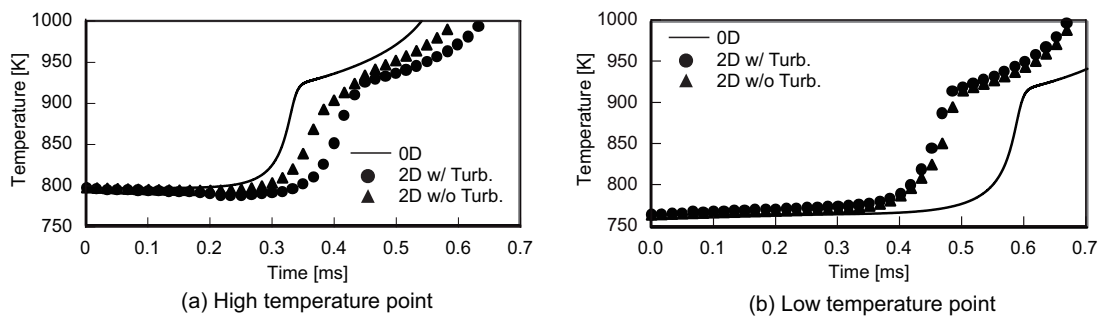
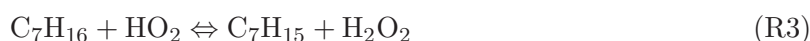
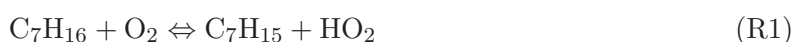


Figure 2: Comparisons of temperature histories at the locations of highest and lowest point in Fig. 1

during the calculation period. The temperature rise at the point H became later than 0D simulation result, and the start of temperature rise at the point L became earlier than 0D simulation result. Furthermore, it was shown that these phenomena under turbulence condition were stronger than static condition. These phenomena were analyzed from the viewpoint of chemical reaction process.

Low temperature oxidation is until the generation of ketohydroperoxide which is relatively stable below the temperature of 850 K, the LTO starts from the generation of the n-heptyl radical as shown below.



At the above-mentioned reactions in n-heptyl radical formation reaction R2, the OH radical has the fastest reaction rate, therefore, OH radical mass is very important. The production and consumption reactions of OH radical in LTO are represented as below.



The reaction rate of 2D DNS was compared with the 0D simulation result with regard to OH production and consumption reaction at the high and low temperature points. Figure 3 shows the comparisons of chemical reaction rates of R2 and from R4 to R8. Chemical reactions for the production of n-heptyl and OH radical in 2D DNS varied as compared with 0D simulation results. It was shown that the start of chemical reaction delayed at the point H. On the contrary, chemical reaction at the point L started at the earlier timing than 0D simulation.

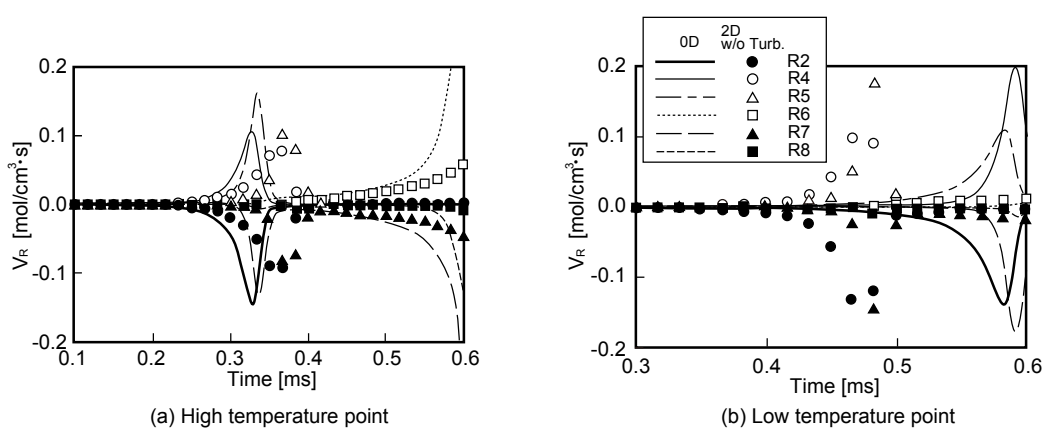


Figure 3: Comparisons of chemical reaction rate to the production and consumption of OH at the high and low temperature points

4 Analysis of the intermediate species diffusion

In this section, the behavior of intermediate species was analyzed at the high and low temperature points H and L. The conservation equation of each chemical species is described below.

$$\frac{\partial \rho Y_m}{\partial t} = -\left(\frac{\partial \rho u_i Y_m}{\partial x_i}\right) + \frac{1}{Pr} \frac{\partial}{\partial x_i} (\rho D_m \frac{\partial Y_m}{\partial x_i}) + \omega_i \quad (1)$$

where Y_m denotes the mass fraction, ω_m is production rate of each chemical species. D_m denotes the effective diffusion coefficients calculated by simplified transport model using Lewis number Le_m of each species.

$$D_m = \frac{\lambda_m}{\rho Le_m c_p} \quad (2)$$

where ρ is density and λ_m denotes the heat thermal conductivity.

The mass flux rate H_m of each chemical species is derived from the advective term and diffusion term of conservation equation (1).

$$k_m = -\left(\frac{\partial \rho u_i Y_m}{\partial x_i}\right) + \frac{1}{Pr} \frac{\partial}{\partial x_i} (\rho D_m \frac{\partial Y_m}{\partial x_i}) \quad (3)$$

$$H_m = \frac{k_m}{\rho Y_m} \quad (4)$$

Here, $H_m < 0$ means mass efflux and $H_m > 0$ is mass influx. Table 3 shows the Lewis numbers of some chemical species. Figure 4 shows the mass flux rate at the points H and L. Figure 5 indicates the history of ratio between the reaction R2 and R4 which are the first consumption and production reaction of OH. A large amount of OH radical which was the smallest Lewis number flowed out from the point

Table 3: Lewis number of each chemical species

N ₂	O ₂	C ₇ H ₁₆	O ₂ C ₇ H ₁₄ OOH	OH	HCHO	H ₂ O ₂
1.00	1.15	3.13	4.07	0.74	1.34	1.14

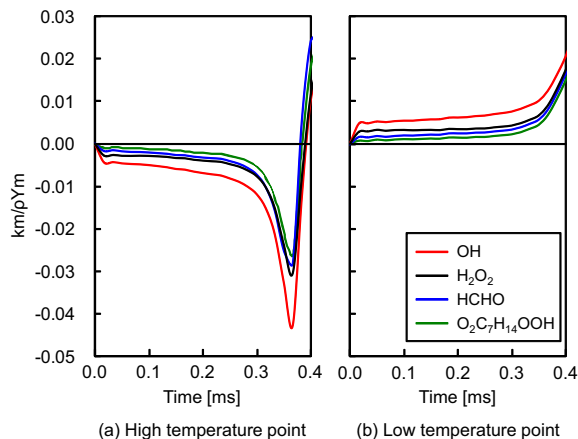


Figure 4: Mass flux histories of each chemical species at the high temperature point H and the low temperature point L

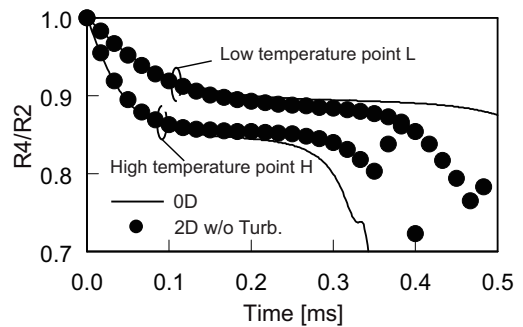


Figure 5: Histories of the ratio of chemical reaction rates between R2 and R4 at the high and the low temperature point H&L

H as compared with other intermediate species. In particular, the efflux of OH radical became larger after 0.2 ms when LTO accelerated, and the reaction R2 was delayed with the increase in OH radical efflux. On the other hand, a large amount of OH radical flowed into the point L, the reaction R2 was enhanced by the increase in OH radical influx after 0.3 ms. It was obvious that the OH radical diffusion made chemical reaction slow, the influx of OH radical from the location where LTO occurs earlier made chemical reaction accelerate.

5 Influence of turbulence on chemical reaction process

In former section, it was indicated that the diffusion of intermediate species made chemical reaction delay, meanwhile, the influx of them made chemical reaction accelerate. Low temperature oxidation under turbulence condition, where the diffusion of chemical species became stronger, was analyzed in this section. OH radical distribution in computational domain, where chemical reaction was promoted, were investigated. Figure 6 shows the comparison of OH radical distribution at each time between with and without turbulence. The history of temperature and the probability density to vorticity is shown in Fig. 7. OH radical increased sequentially, as if the flame propagates, from a high temperature region under non-turbulence condition. Meanwhile, OH radical increased in a wide range due to the transport and diffusion under turbulence condition. In particular, the mass and spatial rate of OH radical increased from 0.3 to 0.4 ms, and it was shown that chemical reaction was promoted and shifted from low temperature oxidation to high temperature oxidation in the high temperature and vorticity.

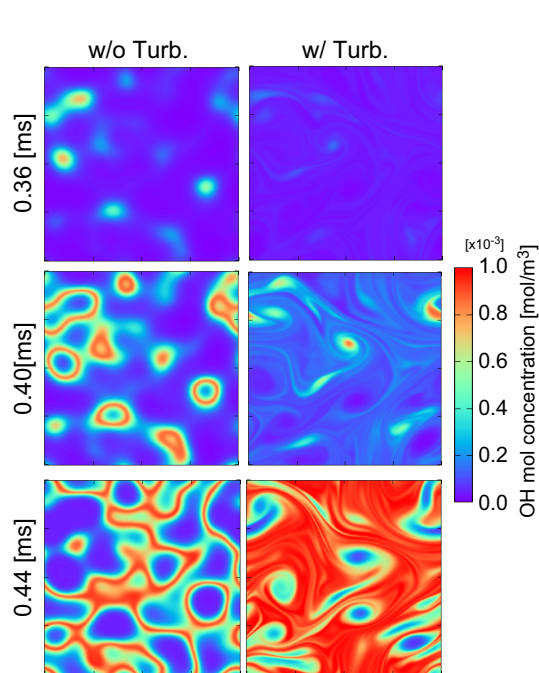


Figure 6: Comparison of OH distribution between with and without turbulence at each time

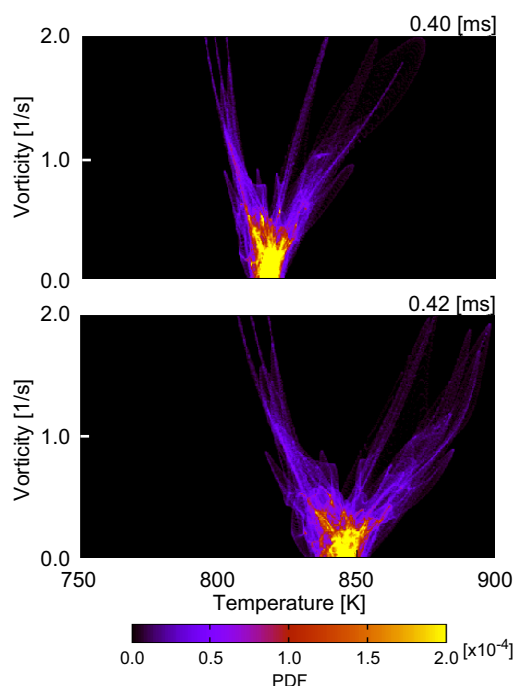


Figure 7: Probability density distributions over temperature and a vorticity at each time

6 Conclusions

The influence of the intermediate specie diffusion on the ignition delay time and chemical reaction process was investigated by making comparison among the 0D numerical analysis and 2D DNS which has with the given temperature distribution. The following knowledge was obtained by performing 2D direct numerical simulation.

1. The diffusion of intermediate species of OH radical makes chemical reaction delay at the high temperature point, and the influx of OH radical from high temperature region makes the chemical reaction promote at the low temperature point.
2. OH radical spreads due to turbulence, and LTO starts in a wide range. Chemical reaction is promoted and shifted from low temperature oxidation to high temperature oxidation in the high temperature and vorticity.

References

- [1] T. Tsurushima, A new skeletal PRF kinetic model for HCCI combustion, *Proceedings of the Combustion Institute*, Vol. 32, No. 2 (2009), pp. 2835–2841.
- [2] C. A. Kennedy and M. H. Carpenter, Several new numerical methods for compressible shear-layer simulations, *Applied Numerical Mathematics*, Vol. 14, No. 4 (1994), pp. 397–433.
- [3] J. S. Shang, High-Order Compact-Difference Schemes for Time-Dependent Maxwell Equations, *Journal of Computational Physics*, Vol. 153, No. 2 (1999), pp. 312–333.
- [4] S. Chapman and T. G. Cowling, The mathematical theory of nonuniform gases(3rd edition), *Cambridge Mathematical Library*, ISBN-13: 978-0521408448 (1991).
- [5] R. X. Yu, X. S. Bai, H. Lehtiniemi, S. S. Ahmed, F. Mauss, M. Richter, M. Alden, L. Hildingsson, B. Johansson and A. Hultqvist, Effect of turbulence and initial temperature inhomogeneity on homogeneous charge compression ignition combustion, *SAE paper*, No. 2006-01-3318 (2006).
- [6] R. X. Yu, X. S. Bai, A. Vressner, A. Hultqvist, B. Johansson, J. Olofsson, H. Seyfried, J. Sjöholm, M. Richter and M. Alden, Effect of Turbulence on HCCI Combustion, *SAE paper*, No. 2007-01-0183 (2007).